AIP | Applied Physics Letters

A tunable coupler for superconducting microwave resonators using a nonlinear kinetic inductance transmission line

C. Bockstiegel, Y. Wang, M. R. Vissers, L. F. Wei, S. Chaudhuri, J. Hubmayr, and J. Gao

Citation: Applied Physics Letters **108**, 222604 (2016); doi: 10.1063/1.4953209
View online: http://dx.doi.org/10.1063/1.4953209
View Table of Contents: http://scitation.aip.org/content/aip/journal/apl/108/22?ver=pdfcov
Published by the AIP Publishing

A tunable coupler for superconducting microwave resonators using a nonlinear kinetic inductance transmission line

C. Bockstiegel,[1,a)] Y. Wang,[1,2,b)] M. R. Vissers,[1] L. F. Wei,[2] S. Chaudhuri,[3] J. Hubmayr,[1] and J. Gao[1]
[1]*National Institute of Standards and Technology, Boulder, Colorado 80305, USA*
[2]*Quantum Optoelectronics Laboratory, Southwest Jiaotong University, Chengdu, Sichuan 610031, China*
[3]*Department of Physics, Stanford University, Stanford, California 94305, USA*

(Received 10 March 2016; accepted 22 May 2016; published online 3 June 2016)

We present a tunable coupler scheme that allows us to tune the coupling strength between a feedline and a superconducting resonator *in situ* over a wide range. In this scheme, we shunt the feedline with a 50-Ω lumped-element nonlinear transmission line made from a 20 nm NbTiN film. By injecting a DC current, the nonlinear kinetic inductance changes and the effective impedance shunting the resonator periodically varies from a short to an open, which tunes the coupling strength and coupling quality factor Q_c. We have demonstrated Q_c tuning over a factor of 40, between $Q_c \sim 5.5 \times 10^4$ and $Q_c \sim 2.3 \times 10^6$, for a 4.5 GHz resonator by applying a DC current less than 3.3 mA. Our tunable coupler scheme is easy to implement and may find broad applications in superconducting detector and quantum computing/information experiments. *Published by AIP Publishing*. [http://dx.doi.org/10.1063/1.4953209]

Superconducting microwave resonators have found important applications in astronomy and quantum computing.[1] They are usually defined lithographically from thin superconducting films. Many resonators with different resonance frequencies may be coupled to a common feedline for multiplexed readout of an array of detectors[2,3] or qubits.[4,5] The coupling strength between the resonators and the feedline, characterized by the coupling quality factor Q_c, is a critical design parameter which sets the photon lifetime in qubit experiments and affects the detector sensitivity of microwave kinetic inductance detectors (MKIDs). Usually, Q_c is fixed by the geometry of the coupling section. In many applications, however, actively tuning the coupling strength and Q_c is desired. For example, a tunable coupler is useful for qubit readout, control,[6,7] and inter-qubit communication.[8,9] The MKIDs would also benefit from a tunable coupler scheme to achieve the critical coupling condition $Q_c = Q_i$, where Q_i is the resonator internal quality factor, to compensate for changes or uncertainty in the optical loading conditions during lab tests and telescope observations.

Previously, a tunable coupler has been demonstrated using a dc-SQUID (superconducting quantum interference device) as the tunable element, which requires Josephson junction fabrication.[10] In this letter, we present a design and experiment for a tunable coupler using a superconducting transmission line with a nonlinear kinetic inductance. This tunable coupler is easy to construct and can tune Q_c of a generic resonator by more than a factor of 40 *in situ*.

Lithographically defined superconducting microwave resonators are photon cavities that store microwave photons. The analogy between a one-sided optical cavity and a 1-port capacitively coupled microwave resonator is illustrated in Figs. 1(a) and 1(b). In both cases, optical (microwave) photons leak in and out of the cavity (resonator) through the partially transparent wall (coupling capacitor) with a transmission coefficient t and associated Q_c given by

$$Q_c = 2\pi \frac{\text{energy stored in cavity}}{\text{energy leaked out per cycle}} = \frac{4m\pi}{|t|^2}, \qquad (1)$$

where m is the optical (electrical) length of the cavity (resonator) in number of wavelengths λ.

In order to tune Q_c, the magnitude of the transmission coefficient $|t|$ has to be varied. Previously, this has been implemented in an inductive coupling scheme, where the mutual inductance controlling the coupling strength is tuned by a flux-biased SQUID circuit.[7,8] In this letter, we describe a tunable capacitive coupling scheme without SQUIDs. In our setup, we shunt the coupling capacitor to ground through a lossless nonlinear transmission line whose phase length is variable, as shown in Fig. 1(c). As the phase length βl is varied, the shunt impedance of the transmission line varies periodically from an open ($\beta l = \pi/2 + n\pi$) to a short ($\beta l = n\pi$), effectively turning the coupling on and off. Here, β is the propagation constant, l is the physical length of the transmission line, and n is an integer. From microwave network analysis, we find that the wave reflected from the transmission line branch interferes with the direct input wave giving rise to a $1 + \gamma_B$ modulation factor on t. The combined coupler

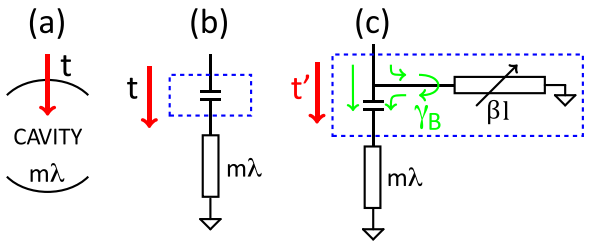

FIG. 1. (a) Cartoon showing an optical cavity, (b) a resonator capacitively coupled to a feedline with one port, and (c) a resonator capacitively coupled to a feedline in the proposed tunable coupler scheme.

[a)]Present address: Department of Physics, University of California Santa Barbara, Santa Barbara, California 93106, USA.
[b)]Electronic mail: qubit@home.swjtu.edu.cn.

block, indicated by the dashed box in Fig. 1(c), has an effective transmission coefficient t' and coupling quality factor Q_c' given by[11]

$$t' = \frac{t(1+\gamma_B)}{2},$$
$$Q_c' = \frac{4Q_c}{|1+\gamma_B|^2} = \frac{Q_c}{\cos^2(\angle\gamma_B/2)} = \frac{Q_c}{\cos^2(\beta l - \pi/2)}, \quad (2)$$

where t and Q_c take the values for the fixed coupler case in Fig. 1(b), and the reflection coefficient $\gamma_B = e^{i\angle\gamma_B} = -e^{-2i\beta l}$ from the terminated lossless transmission line is assumed. Eq. (2) clearly suggests that the effective Q_c' of the tunable coupler may be continuously tuned from the original Q_c to infinity by varying the phase length of the transmission line.

To vary the phase length, we introduce a lumped-element transmission line with nonlinear kinetic inductance made from 20 nm NbTiN. NbTiN has a current-dependent kinetic inductance, modeled by

$$L_k = L_{k,0}\left[1 + \left(\frac{I}{I_*}\right)^2\right], \quad (3)$$

where I is the current flowing through the inductor and I_* is a characteristic current on the order of the superconducting critical current.[1] The nonlinear kinetic inductance of NbTiN has been found to exhibit extremely low dissipation and used in the construction of nonlinear superconducting devices, such as broadband traveling-wave parametric amplifiers,[12,13] frequency tunable resonators,[14] and frequency combs.[17] In this experiment, we adopt a lumped-element transmission line design that is modified from a conventional coplanar waveguide (CPW) transmission line. We place 2 μm interdigitated capacitor (IDC) fingers directly on both sides of the 2 μm center strip, forming a "fishbone" pattern as shown in Fig. 2. The added capacitance to ground compensates for the high kinetic inductance of the NbTiN center strip resulting in a lumped element transmission line with characteristic impedance of $Z_0 = 50\ \Omega$, naturally matched to the measurement system. For the design parameters shown in Fig. 2, we have verified $Z_0 = 48.5\ \Omega$ with time-domain reflectometry (TDR) measurements in an LHe dunk test. As a comparison, a CPW made from 20 nm NbTiN with 2 μm center and gap would have an impedance of more than 200 Ω. It should be pointed out that the tuning element is not limited to a 50 Ω transmission line and in general any lossless component with a variable reactance may work as a tunable coupler. However, in other impedance mismatched cases, the phase of the reflection coefficient oscillates rapidly with frequency, limiting it to be useful only for narrow-band devices. The trade-off for the 50 Ω fishbone tuner is that the overall footprint is increased by about a factor of 3 from a meandered CPW implementation due to the added IDC fingers. The footprint is not significantly increased, thanks to the fact that the added IDC also reduces the phase velocity and the required length of the fishbone line by a factor of 4 from the CPW counterpart.

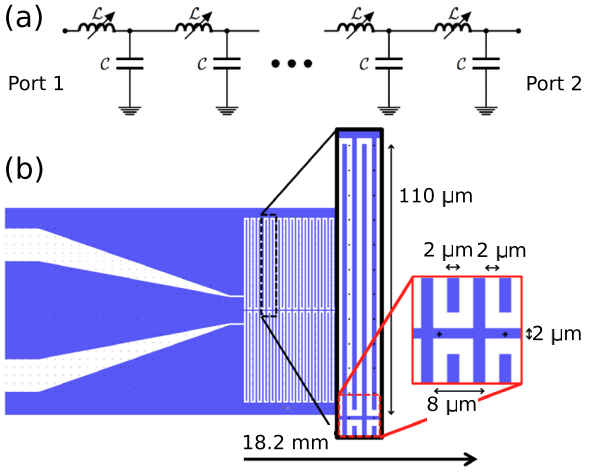

FIG. 2. (a) Lumped element model of a nonlinear kinetic inductance transmission line where the inductance L depends on the current I. (b) One port of the "fishbone" nonlinear transmission line with IDC features. The design dimensions listed in the figure yield a transmission line close to 50 Ω characteristic impedance. NbTiN is shown in blue and exposed substrate in white.

Because the propagation constant is related to the nonlinear inductance by $\beta = \omega\sqrt{L(I)C}$, the phase length may be modulated by a DC current (I_{dc})

$$\beta l = \beta_0 l\left[1 + \frac{\alpha}{2}\left(\frac{I_{dc}}{I_*}\right)^2\right], \quad (4)$$

where $\beta_0 l$ corresponds to the phase length at zero current and α is the kinetic inductance fraction.[1] Therefore, we have constructed a lossless transmission line whose phase length can be varied by injecting a DC current (neglecting the effect of a slight impedance change[11]), as required by the tunable coupler scheme in Fig. 1(c).

Our Q_c tuning experiment was conducted using the setup shown in Fig. 3 in an adiabatic demagnetization refrigerator (ADR) maintained at a bath temperature of 380 mK, well below the superconducting transition temperature of the rhenium resonators ($T_c \sim 1.7$ K) and the NbTiN fishbone

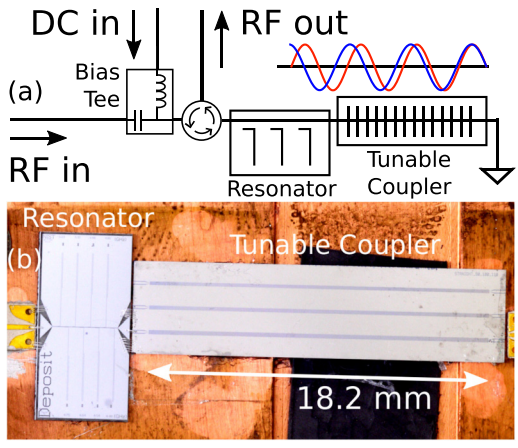

FIG. 3. (a) A diagram showing the tunable coupler setup. The DC current is injected through the bias tee and flows through the circulator, resonator feedline, fishbone transmission line, and finally through a short to ground. A larger DC current reduces the wavelength of the standing wave (illustrated by the red and blue sinusoidal waves) and varies the phase of the wave seen by the resonator. (b) Photograph of the resonator chip (left) and fishbone transmission line (right). One of the eight resonators on the resonator chip and one of the three fishbone transmission lines were used in our experiment.

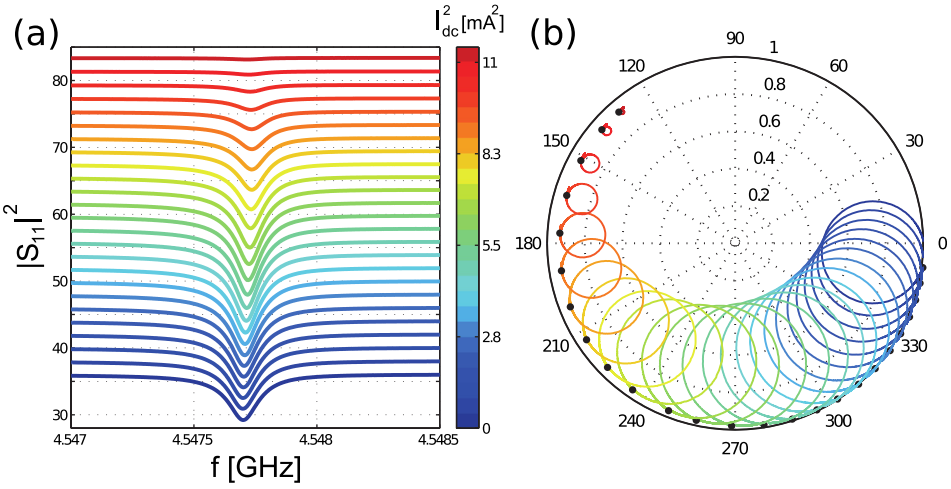

FIG. 4. Network analyzer sweeps of the resonator-coupler circuit for different values of DC current. $|S_{11}|^2$ data are plotted in (a) with 2 dB offsets in the y-axis added for clarity. The resonance frequency is mostly unchanged but the depth of the resonance dip is modulated by varying Q_c. The normalized complex S_{11} data are plotted in (b). The diameter of the resonance circle is modulated by the effective coupling, Q_c. The first (lowest) frequency point in each sweep is indicated by the black dots.

transmission line ($T_c \sim 14$ K). A battery-powered, low noise voltage supply provided a DC current, which was injected into the feedline using a bias tee and a 1 kΩ series resistor. This DC current flows through the circulator, resonator feedline, fishbone transmission line, and finally through a short to ground. The output RF signal, the S_{11} reflection from the entire network including the resonator and the lumped transmission line, was amplified with a HEMT at 3 K. The center-to-ground short at one end of the fishbone transmission line and the interconnections between the resonator chip and the fishbone transmission line chip were made using aluminum wirebonds.

We first measured the device reflection around its resonance frequency of 4.548 GHz using a vector network analyzer (VNA), while DC current injected into the fishbone transmission line was stepped from 0 to a maximum value of $I_{max} = 3.32$ mA. For $I > I_{max}$ part of the transmission line went normal, and the transmission was dramatically reduced. Fig. 4(a) shows a waterfall plot of all the measured $|S_{11}|^2$ curves under different bias currents. One can see that with the increasing DC current, the resonance dip first goes deeper and then shallower, indicating the coupling quality factor Q_c of the resonator is effectively tuned by the DC currents.

To further analyze the reflection data, we normalized the complex S_{11} data at 380 mK for different DC currents to the S_{11} data with no injected DC current at 700 mK. At 700 mK, the resonances die out due to thermal quasiparticles, leaving a clean background for reference. This normalization technique removes cable delays and losses from coaxial cables and was commonly used in resonator measurements in Ref. 15.

The normalized resonance loops for all the DC currents are shown in Fig. 4(b). The diameter of each resonance loop is directly related to its effective coupling quality factor, Q_c'. With increasing DC current, the centers of the resonance loops move clockwise and the diameters change, indicating both the phases of S_{11} and Q_c' change with current. The black dots in Fig. 4(b) indicate the first frequency point f_1 in each sweep. Measured at a fixed off-resonance frequency f_1, $\gamma_B \approx S_{11}(f_1) = e^{i\theta}$ gives the reflection coefficient (normalized) from the nonlinear fishbone transmission line only. The phase of these black dots, θ, versus DC current squared, I_{dc}^2, is plotted in Fig. 5(a). According to Eq. (4), $\theta \propto I_{dc}^2$. The θ vs. I_{dc}^2 curve roughly follows a linear trend but at higher currents a clear departure is visible. This effect has been previously observed in other nonlinear devices using NbTiN, where a quartic term I_{dc}^4 has to be included to fit the data.[14,16] Such a quartic term may arise from higher order nonlinear response of kinetic inductance or from quasiparticle generation.[14] Despite the detailed model of $\theta(I_{dc})$ and its underlying physics, Fig. 5(a) shows that we have obtained a large nonlinear phase shift of over π useful for Q_c tuning by injecting a DC current.

To quantitatively assess the Q_c tunability, we retrieve the effective Q_c' for each value of I_{dc} by fitting the complex S_{11} data to a theoretical model derived for our circuit configuration,[11]

$$S_{11}(f) = \gamma_B \left[1 - \frac{2Q/Q_c'}{1 + i2Q\left(\frac{f - f_r}{f_r}\right)} \right], \tag{5}$$

using the established resonator fitting procedure outlined in Ref. 15. Here, f_r and Q are the resonance frequency and total quality factor, respectively. Fig. 5(b) shows the fitted Q_i (squares) and Q_c' (dotted) plotted against I_{dc}^2. The internal loss Q_i remains nearly constant with increasing DC current while Q_c' ranges from a minimum $Q_{c,min} = 5.5 \times 10^4$ at $I_{dc} = 2.14$ mA to a maximum $Q_{c,max} = 2.3 \times 10^6$ at $I_{dc} = 3.32$mA. This result clearly demonstrates that we have achieved tuning of Q_c by

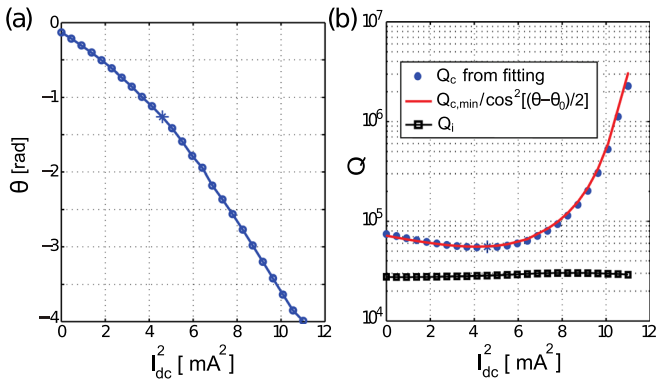

FIG. 5. (a) Current-induced nonlinear phase shift θ and (b) quality factors as a function of DC current squared I_{dc}^2. The minimum $Q_{c,min}$ and the correspondent nonlinear phase shift θ_0 are indicated by the stars.

more than a factor of 40, while Q_i is unaffected. We further infer that when $Q_{c,\min}$ is reached the DC current has induced an additional nonlinear phase $\theta_0 \sim 1.25$ rad in the transmission line, making the total phase length $\beta l = \pi/2 + n\pi$.

In order to check the agreement between our model and our data, we plot the theoretical model implied by Eq. (2), $Q_c' = Q_{c,\min}/\cos^2[(\theta - \theta_0)/2]$, where θ is the current induced nonlinear phase shift given by Fig. 5(a), $Q_{c,\min}$ is the lowest measured Q_c' and θ_0 is its corresponding nonlinear phase (indicated by the stars in Fig. 5). As shown by the red curve in Fig. 5(b), the theoretical model is in excellent agreement with the measured Q_c'.

In conclusion, we have demonstrated the tunable coupler scheme for superconducting microwave resonators proposed in Fig. 1(c) and achieved Q_c tuning over a factor of 40, from $Q_c \sim 5.5 \times 10^4$ to $Q_c \sim 2.3 \times 10^6$. Our scheme uses the current-dependent nonlinear kinetic inductance in a superconducting NbTiN transmission line without any Josephson junctions. We have introduced a lumped-element transmission line architecture with an interdigitated capacitor to compensate for the high kinetic inductance of NbTiN. We have constructed such a transmission line with 50 Ω intrinsic characteristic impedance, which provides an elegant solution to transmission line designs using high kinetic inductance films for other applications, such as kinetic inductance traveling-wave parametric amplifiers. This device is easy to construct and requires only single layer fabrication. Integrating the tunable coupler with the resonators to be tuned onto the same chip should be straightforward. If a tight integration is needed, the footprint of the coupler circuit can be further reduced by shrinking the width of the spine and the IDC finger/gap of the fishbone. The demonstration described here was for a 1-port resonator; it is straightforward to extend the scheme to 2-port resonators with independent control of the coupling strength for the two ports.

The devices were fabricated in the NIST cleanroom. Yiwen Wang was supported in part by the National Natural Science Foundation (Grant No. 61301031) and the Fundamental Research Funds for the Central Universities (Grant No. 2682014CX087).

[1]J. Zmuidzinas, Annu. Rev. Condens. Matter Phys. **3**, 169 (2012).
[2]P. K. Day, H. G. LeDuc, B. A. Mazin, A. Vayonakis, and J. Zmuidzinas, Nature **425**, 817 (2003).
[3]K. D. Irwin and K. W. Lehnert, Appl. Phys. Lett. **85**, 2107 (2004).
[4]J. Kelly, R. Barends, A. G. Fowler, A. Megrant, E. Jeffrey, T. C. White, D. Sank, J. Y. Mutus, B. Campbell, Y. Chen *et al.*, Nature **519**, 66 (2015).
[5]N. G. Dickson, M. W. Johnson, M. H. Amin, R. Harris, F. Altomare, A. J. Berkley, P. Bunyk, J. Cai, E. M. Chapple, P. Chavez *et al.*, Nat. Commun. **4**, 1903 (2013).
[6]M. S. Allman, F. Altomare, J. D. Whittaker, K. Cicak, D. Li, A. Sirois, J. Strong, J. D. Teufel, and R. W. Simmonds, Phys. Rev. Lett. **104**, 177004 (2010).
[7]M. S. Allman, J. D. Whittaker, M. Castellanos-Beltran, K. Cicak, F. da Silva, M. P. DeFeo, F. Lecocq, A. Sirois, J. D. Teufel, J. Aumentado *et al.*, Phys. Rev. Lett. **112**, 123601 (2014).
[8]Y. Yin, Y. Chen, D. Sank, P. J. J. O'Malley, T. C. White, R. Barends, J. Kelly, E. Lucero, M. Mariantoni, A. Megrant *et al.*, Phys. Rev. Lett. **110**, 107001 (2013).
[9]J. Wenner, Y. Yin, Y. Chen, R. Barends, B. Chiaro, E. Jeffrey, J. Kelly, A. Megrant, J. Y. Mutus, C. Neill *et al.*, Phys. Rev. Lett. **112**, 210501 (2014).
[10]R. Harris, A. J. Berkley, M. W. Johnson, P. Bunyk, S. Govorkov, M. C. Thom, S. Uchaikin, A. B. Wilson, J. Chung, E. Holtham *et al.*, Phys. Rev. Lett. **98**, 177001 (2007).
[11]See supplementary material at http://dx.doi.org/10.1063/1.4953209 for detailed network analysis of the circuit.
[12]B. Ho Eom, P. K. Day, H. G. LeDuc, and J. Zmuidzinas, Nat. Phys. **8**, 623 (2012).
[13]C. Bockstiegel, J. Gao, M. R. Vissers, M. Sandberg, S. Chaudhuri, A. Sanders, L. R. Vale, K. D. Irwin, and D. P. Pappas, J. Low Temp. Phys. **176**, 476 (2014).
[14]M. R. Vissers, J. Hubmayr, M. Sandberg, S. Chaudhuri, C. Bockstiegel, and J. Gao, Appl. Phys. Lett. **107**, 062601 (2015).
[15]J. Gao, Ph.D. thesis (California Institute of Technology, 2008).
[16]A. Kher, P. K. Day, B. H. Eom, J. Zmuidzinas, and H. G. Leduc, J. Low Temp. Phys. **184**(1–2), 480 (2015).
[17]R. P. Erickson, M. R. Vissers, M. Sandberg, S. R. Jefferts, and D. P. Pappas, Phys. Rev. Lett. **113**, 187002 (2014).